Pergamon

Int. J. Heat Mass Transfer. Vol. 37, Suppl. 1, pp. 73–82, 1994

0017-9310/94 $6.00 + 0.00

0017-9310(93)E0057-N

Experimental investigation on liquid forced-convection heat transfer through microchannels†

B. X. WANG and X. F. PENG
Thermal Engineering Department, Tsinghua University, Beijing 100084, China

Abstract—Experiments were conducted to investigate the single-phase forced-flow convection of water or methanol flowing through microchannels with rectangular cross-section. The fully developed turbulent convection regime was found to be initiated at about $Re = 1000$–1500. The fully developed turbulent heat transfer can be predicted by the well-known Dittus–Boelter correlation by modifying the empirical constant coefficient from 0.023 to 0.00805. The calculated results are then in quite good agreement with experimental data. The transition and laminar heat transfer behavior in microchannels are very unusual and complex and are strongly affected by liquid temperature, velocity and microchannel size.

1. INTRODUCTION

BECAUSE of its extraordinary advantage for practical applications, microfabrication or nanotechnology, originally emerging from the technology developed for integrated circuits, has expanded rapidly into such fields as bioengineering and biotechnology, aerospace, mini heaters and mini heat exchangers, electronics and microelectronics, materials processing, and thin film deposition technologies, and has resulted in remarkable contributions to the development of modern high technology. Moreover, it may provide new tools for examining physical phenomena, and supply new possibilities for experimentally studying and measuring the thermal phenomena that are difficult to measure in usual situations [1].

The analyses of heat transfer phenomena in the above-mentioned applications and new technological developments offer new and unique areas of research. For example, owing to the urgent needs for cooling electronic components and devices, microscale heat transfer technologies such as mini heat exchangers with flow channels having dimensions ranging from the order of several hundred to 0.1 micrometers have been developed. These microchannels and mini heat exchangers have found their application in reactors for modification and separation of biological cells, selective membranes and liquid/gas chromatographies. As pointed out by Yang and Zhang [2], the last decade of the twentieth century may witness rapid progress in research of microscale and nanoscale transport phenomena. Microscale heat transfer and transport phenomena are expected to be quite different from those in customary situations. It is absolutely necessary to understand these phenomena so as to develop related new high technologies, and tremendous challenges and opportunities are envisioned to conduct theoretical and experimental research on the fundamentals of heat transfer at the microscale level.

Tuckermann and Pease [3, 4] demonstrated that the electronic chip can be effectively cooled by means of water flow in microchannels fabricated on the circuit board on which the chips are mounted. Their results also indicated that the heat transfer coefficient of laminar flow through microchannels might be higher than that of turbulent flow through normally sized channels. Wu and Little [5], Pfahler *et al.* [6], and Choi *et al.* [7] noted that the flow and heat transfer characteristics of fluid through microchannels or microtubes departs from the thermofluid experimental results for convectional-sized channels. These investigations provided substantial experimental data and considerable insight into some behaviors of the heat transfer and fluid flow in microtubes without phase change. The studies conducted for the microscale heat transfer with phase changes are limited only for micro heat pipes [8–10], microconvection and evaporation in sessile drops [11–13] and augmentation of boiling heat transfer on composite surfaces [14, 15]. Until now, there have been few investigations of the flow boiling of liquid through microchannels or microtubes reported in the literature. Peng and Wang [16, 17] recently conducted experiments to investigate the single phase and forced-flow convection and boiling characteristics of subcooled liquid through rectangular cross-section microchannels of 0.6×0.7 mm. These experiments indicated that the single-phase convection and flow boiling are distinct from those through normally sized tubes and channels, and their heat transfer was augmented. The boiling was initiated earlier and no apparent partial nucleate boiling lasted for subcooled liquid in microchannels.

In the present work, our attention focused on con-

†Dedicated to Professor James P. Hartnett on his 70th birthday.

NOMENCLATURE

A_1	area of the sides of microchannel
A_2	area of the bottom of microchannel
d_h	effective diameter
Gr	Grashof number
h	heat transfer coefficient
H_c	height of microchannel
I	current
k	conductivity
L	length of microchannel
N	number of microchannel
Pr	Prandtl number
Re	Reynolds number
Q	total applied power
q''	heat flux
r	modification coefficient accounting for heat loss
T	temperature
T_i	temperature sample, $i = 1, 2, 3, \ldots$
U	voltage
u	flow velocity
W	width of test plate
W_c	width of microchannel
W_t	distance between two microchannels.

Greek symbols

μ	dynamical viscosity
ν	viscosity.

Subscripts

f	liquid
w	wall.

ducting a series of experiments to explore convective heat transfer of liquid through microchannels, and understand some physical phenomena and essential fundamentals. Attempts were also made to inspect experimentally the influence of liquid flow and thermal parameters, geometrical size and structure on single phase forced-convective heat transfer characteristics for subcooled liquid flow through microchannels.

2. TEST FACILITY AND EXPERIMENTAL DESCRIPTION

The test facility was set up as shown schematically in Fig. 1. It consists of a liquid pool, liquid pump, test section and control valves for adjusting the flow rate. The liquid temperature in the pool was kept constant by different valves for heating or cooling. Liquid was pumped into the circuit line where part of it flowed through the test section and returned to the pool and part flowed through the by-pass tube line to the pool. With this experimental system/set-up, it was very convenient to adjust the flow rate and maintain a steady liquid flow rate. An open-loop system was chosen for this investigation and the flow rate was determined by the weighing method.

The microchanneled structures to be tested were made of stainless steel plate, 18 mm wide and 125 mm long, on which several microchannels were machined in parallel. Figure 2 is a schematic diagram showing details of the test section. The thickness of the region of the plate where the microchannels were machined was 2 mm. The tested length of the microchannel was 45 mm. There were six kinds of microchanneled structures utilized in this investigation. Each microchannel cross-section was rectangular with different widths and identical channel height of 0.7 mm. There were N (4 or 6) microchannels with identical geometries evenly distributed on each test plate. The geometrical parameters of the tested microchanneled structures are summarized in Table 1.

Thermocouples for measuring liquid temperature were located at the inlet and outlet of the test section. In addition, six thermocouples were mounted on the back of the microchannel plate, three thermocouples at the upstream end and another three at the down-

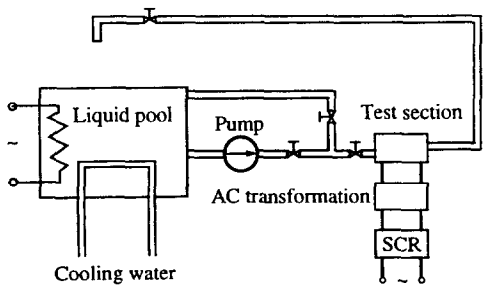

FIG. 1. Test facility.

Table 1. Geometric parameters of test section

Test section	L (mm)	W (mm)	W_c (mm)	W_t (mm)	H_c (mm)	N
No. 1	45	18	0.8	3.4	0.7	4
No. 2	45	18	0.6	3.6	0.7	4
No. 3	45	18	0.4	3.8	0.7	4
No. 4	45	18	0.4	2.4	0.7	6
No. 5	45	18	0.2	4.0	0.7	4
No. 6	45	18	0.2	2.6	0.7	6

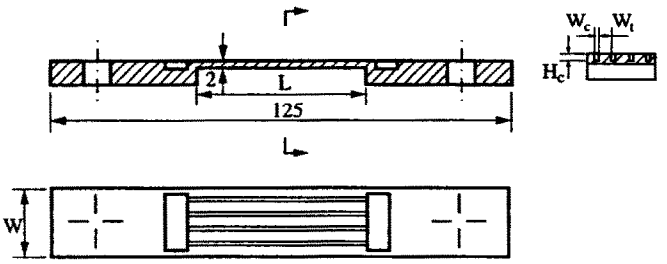

FIG. 2. Test section (dimensions in mm).

stream end, to measure the plate wall temperature. The stainless steel plate on which the microchannels were machined was electrically heated by directly connecting the plate to an AC electrical-current transformer matched with an SCR voltage regulator that provided low voltage and high electric current. Hence, high, uniform heat flux was supplied along the test section. The input voltage and current were adjusted to control the applied heat flux. By this heating method, the heat was generated in the microchanneled plate, which may be a better way to simulate the heat generated by electronic components.

Methanol and deionized water were employed as the working fluids. The working liquid temperature varied from 10°C to 35°C for water and 14–19°C for methanol, i.e. the liquid subcooling varied from 65°C to 90°C for water at ambient pressure. The liquid velocity varied from 0.2 to 2.1 m s^{-1} to obtain the specified liquid velocity and subcooling condition. For each test, the system was allowed to reach steady state. Then the corresponding liquid flow rate, liquid and plate wall temperatures, and the voltage and current were measured and recorded.

3. DATA PROCESSING AND UNCERTAINTY

Data reduction

For the data processing, the plate temperature was corrected from the measured temperature on the back of the plate to the bottom surface temperature of the microchannel. The surface temperature of all three heated sides was assumed to be uniform for the tested cases here. This presumption was confirmed to be reasonable by numerically analyzing the effect of local variation in the heat flux and temperature distributions. The flow rate and velocity through the microchannels were the averages as calculated from the measured mass flow of all four or six microchannels. It was much more complicated to determine the actual heat flux from the side surfaces of the microchannel to the liquid flow, because all microchannels were machined on the heating plate, so that the thickness of the heating plate was not uniform. This resulted in heterogeneous heat generation of the heating plate. Consequently, the applied heat fluxes, from the three sides of the channel except the top cover plate surface, were not uniform. Considering this heterogeneity, great care was taken to design the distribution of the microchannels on the plate as shown in Fig. 2 and to manufacture them accordingly. The test inspection [16] and corresponding numerical analysis [17] indicated that this distribution ensured that the applied heat flux from the microchannel sides was rationally uniform. Hence, the applied surface heat flux can be calculated from total input power as

$$q'' = \frac{Q}{N(2A_1 + A_2)}, \tag{1}$$

where A_1 and A_2 are the area of the side and the bottom of the channel, respectively. The total applied power heat generation was determined from the measured current, I, and the voltage, U, i.e.

$$Q = rIU. \tag{2}$$

The heat flux at the wall surface in equation (1) was calculated by subtracting conduction and other heat losses from the power supplied, and was verified by comparing it to the sensible heat gained by the liquid between the inlet and the outlet. The conductive and other heat losses were estimated assuming natural convection on the outside surface of the insulation wrapped around the test section under steady-state flow conditions without phase change. The modification coefficient, r, in equation (2) accounts for all these heat losses and was determined from the experimental energy balance. The measured and calculated net heat fluxes had a variation of less than $\pm 3.0\%$. The measurement of the plate surface temperature and the experimental observations also showed that there exists no observable difference between the fluid flow and heat transfer characteristics in different microchannels on test plates. This implies that the method of data processing employed is reasonably acceptable. We will, therefore, discuss measured results for one microchannel only as the representation.

The local heat transfer coefficients were evaluated as

$$h(x) = \frac{q''}{[T(x) - T_f]}, \tag{3}$$

where T_f denotes the liquid temperature measured at

the inlet. $T(x)$ was determined from the three wall temperatures measured at the same x position along the flow direction. For convenience, in the present study, the heat transfer coefficient was calculated at the downstream end of the microchannels. Final data were reduced in terms of Nusselt number,

$$Nu = \frac{h(x)D_h}{K_f} \tag{4}$$

and Reynolds number,

$$Re = \frac{uD_h}{\nu_f} \tag{5}$$

Uncertainty analysis

To estimate the uncertainties in the applied wall heat flux and the heat transfer coefficients, we have from equations (1) and (2)

$$q'' = \frac{rIU}{N(2A_1 + A_2)}. \tag{6}$$

Combining equations (3) and (6) yields

$$h(x) = \frac{rIU}{N(2A_1 + A_2)[(T_1 + T_2 + T_3)/3 - T_f]}, \tag{7}$$

where T_1, T_2, and T_3 are the temperatures from the three thermocouples mounted on the back of the plate near the upstream or downstream end. The uncertainties of both the current and voltage measurements were within 0.2%. The errors in the dimension measurements were less than 1%. Type-T (copper–constantan) thermocouples with an accuracy of 0.4% were utilized to measure both fluid and wall temperatures. The thermocouple read-out uncertainty was 0.3%. Other uncertainties were estimated as follows: 2% for the average wall temperature which indicates the variation in the read-out from the three thermocouples, 2% for the AC current and voltage due to small fluctuations, 1.5% for the flow rate, and 2.5% for the liquid velocity. The maximum uncertainty for the heat transfer coefficient, $h(x)$, is 6%. The random uncertainties of Nusselt and Reynolds number are expected to be less than 8% and 5%, respectively.

4. EXPERIMENTAL RESULTS AND DISCUSSIONS

Figure 3 illustrates the experimental results of water convective heat transfer for all tested microchanneled plates, actually the variation of heat transfer coefficients with microchannel surface temperature. Obviously, some data of flow nucleate boiling heat transfer, included in Figs. 3(a)–(c), are not dealt with in the following discussions. Generally speaking, heat transfer is augmented as liquid temperature recedes and liquid velocity increases. All the experimental measurements support this conclusion. However, there exist some differences in the change of heat transfer coefficient, h, with surface temperature, T_w, in different experiments. The heat transfer coefficient in Fig. 3(a) monotonously and smoothly increases with wall surface temperature, while the data in Figs. 3(b)–(d) exhibit a steep enhancement in heat transfer coefficient prior to the zone of monotonous and smooth rise in the coefficient. In Figs. 3(e) and (f), the variation of the heat transfer coefficient could be divided into three situations: the region on the left side of the graph in which the coefficient decreases, the middle area where steep enhancement occurs, and the zone of generally monotonous and smooth rise in the coefficient. Even for the generally monotonous and smooth rise zone, analyses and comparisons indicated that the rise of heat transfer coefficient with surface temperature is restrained as microchannel size diminishes. Explicitly, the slope of the h–T_w curve gradually alters and becomes smaller from the circumstance in Fig. 3(a) to that in Figs. 3(b)–(e), and finally Fig. 3(f). In addition, both liquid velocity and temperature have significant influence on the characteristics of the h–T_w curve. Increasing liquid flow velocity provokes the steep enhancement of the coefficient and the transition is shifted to the left, as shown in Figs. 3(d) and (e). For generally monotonous and smooth rise zone, increasing liquid velocity and/or reducing liquid temperature causes the slope of h–T_w to dwindle, as illustrated in Figs. 3(b) and (c).

Basically, the behavior of heat transfer coefficient is highly associated with liquid flow or heat transfer mode, and the variation in Fig. 3 implies that there exist separate heat transfer mechanisms accordingly. We have previously discussed similar observed phenomena [16–18]. Reasonably, laminar flow might be expected prior to the transition, and the transition might be where the laminar liquid flow and heat transfer tend to become turbulent. Because of the extremely small channel, the heating creates a large change in the liquid temperature. As a consequence, the thermophysical properties of the flowing liquid change dramatically. For example, the Reynolds number, Re, for the experiments using the microchanneled structures was usually about 500–1000 at the inlet, and about 1800–2500 or larger at the outlet for the range of water flow velocities and other experimental conditions used. This means that for water flow, the Reynolds number could be possibly doubled over the length of the microchannel for an inlet Reynolds number of only around 1000. Clearly, variations in the heating rate or wall temperature induce relatively large changes in the Reynolds number. For fluids flowing through microchannels, Wu and Little [5] found transition to turbulence at much lower Reynolds number than that of conventional-sized channels. We may conclude, therefore, that the experimental results in Fig. 3 are a consequence of the large increase in the wall surface temperature.

The experimental results of Nusselt number, Nu, are plotted vs Reynolds number, Re, for water in Fig. 4, and for methanol [18] in Fig. 5. The experiments previously conducted on methanol, with test sections

No. 3–6 only, have been reported in ref. [18]. When Re is greater than about 1500, all data taken from different text sections fall close to a single straight line on the log–log graph. For $70 < Re < 1500$, some data also fall along the same line, while some data fall above the line. For $Re < 700$, the relationship between Nu and Re is quite complex, and Nu is a function of other variations besides Re. These will be discussed later.

The data distribute within the straight belt zone like those of turbulent convective heat transfer. Wu and Little [5] suggested a heat transfer correlation for gas flow through microchannels for $Re > 3000$, i.e. turbulent flow zone, as

$$Nu = 0.00222Pr^{0.4}Re^{1.09}. \quad (8)$$

Compared with the prediction by equation (8), the data obtained here are much smaller and the variation of Nu as a function of Re is distinct from that predicted by equation (8). However, the well-known heat transfer correlations of a normally sized channel for fully developed turbulent flow,

$$Nu = 0.023Re^{4/5}Pr^{1/3}, \quad (9)$$

gives very good agreement in the Nu–Re variation regularity; the predicted values are still much larger than the experimental data. If the empirical coefficient, 0.023, is replaced with 0.00805, or equation (9) is modified as

$$Nu = 0.00805Re^{4/5}Pr^{1/3}, \quad (10)$$

the experimental data match the predicted results very well, as shown in Fig. 4. This implies that fully turbulent flow is induced much earlier with Re of only about 1000–1500 for liquid flow in microchannels, compared with conventional situation. Apparently, the transition region to turbulent flow is not restricted in the range of sharp enhancement in heat transfer coefficient as noted above.

The experimental data deviating from the results calculated by equation (10) and of $Re < 800$ are likely in the mixing convective dominion, as conventional forced convection, and/or aforementioned transition heat transfer. For liquid forced flow through a normally sized channel, buoyancy-driven flow becomes significant and mixing convective heat transfer takes place when the Grashof number, Gr, reaches a critical value or $Gr/Re^2 \approx 0.1$ [17]. Under the conditions of the experiments conducted, the Grashof number is less than 800 or, correspondingly, Gr/Re^2 is less than 0.005, and therefore, free convection effects would be neglected and only forced convection applies; this is transition individuality of forced convection in microchannels. This variation or transition is extremely unusual.

To explore the behavior of heat transfer in the transition region and the influences of flow, thermal and geometrical parameters, experimental data obtained for different test sections are separately plotted in Fig. 5. Because the data of the test section No. 1 can be correlated by equation (10) and no transition phenomenon was found for this case, as shown both in Figs. 3(a) and 4, these results are not illustrated in Fig. 5. Comparing Fig. 3(b) with Fig. 5(a), Fig. 3(c) with Fig. 5(b), and Fig. 3(d) with Fig. 5(c), the data on the $h - T_w$ curves with smaller or nearly zero slope departing from equation (10) are in the transition zone. When the deviation or transition appears, Nu is almost independent of Re for a given liquid velocity and inlet temperature as h does not depend upon T_w in Fig. 3. Then, Nu sharply goes down with decrease of Re where the transition region may be going to terminate and a new heat transfer mode may take place. There are some differences in Fig. 5(d). Corresponding to Figs. 3(e) and (f), there are three different regions similar to those discussed above. Prior to the transition zone, Nu recedes with Re. This is expected to be the laminar flow zone. There is a very narrow area in which flow is altered from the laminar to the transition regime. Nu is approximately not affected by the increase of Re after transition has occurred. The latter is referred to as the transition zone as in other cases; however, Nu is smaller.

Figure 6 shows that the effects of liquid velocity, inlet liquid temperature and geometrical parameter for water on the transition and laminar region are apparent and of significant importance. From Figs. 3(a) and 6(a)–(c), higher inlet liquid temperature and liquid velocity promote fully developed turbulent heat transfer. Decreasing liquid velocity and increasing liquid temperature, the transition to fully turbulent flow occurs at lower Re and the transition zone in which Nu is nearly constant is enlarged. The results in Fig. 6(d) display identical changes. The transition from the laminar to transition heat transfer mode is also relative to liquid temperature and velocity. It surfaces at greater Re when liquid temperature is higher and velocity larger. By comparing the results of different test sections, all these phenomena are observed at lower Re as microchannel size becomes smaller for specified liquid velocity and temperature. It is necessary to investigate further these influences, both experimentally and analytically.

5. CONCLUSIONS

The single-phase forced convective heat transfer characteristics of water/methanol flowing through microchannels with rectangular cross-section were experimentally investigated. The results provide significant data and considerable insight into the behavior of the forced-flow convection in microchannels. They show that liquid convection characteristics are quite different from those of the conventional cases and can be summarized as follows.

(1) For single-phase liquid forced convection through microchannels, a fully developed heat transfer regime is initiated at about $Re = 1000$–1500. The transition to turbulent mode is influenced by liquid temperature, velocity and microchannel size. The well

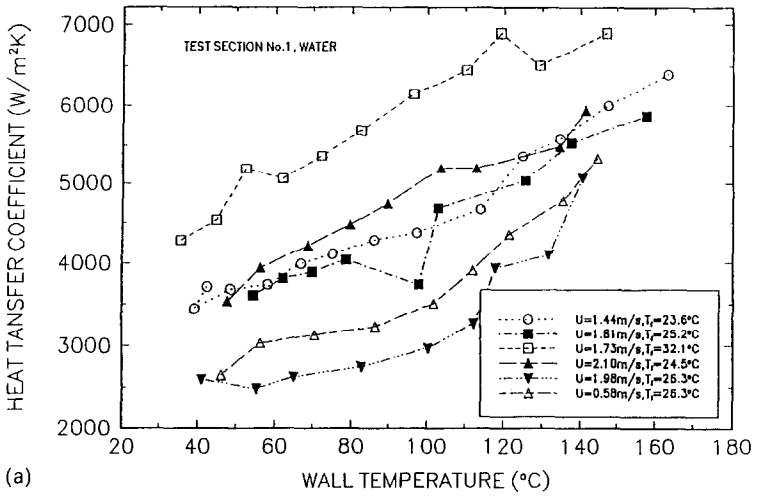

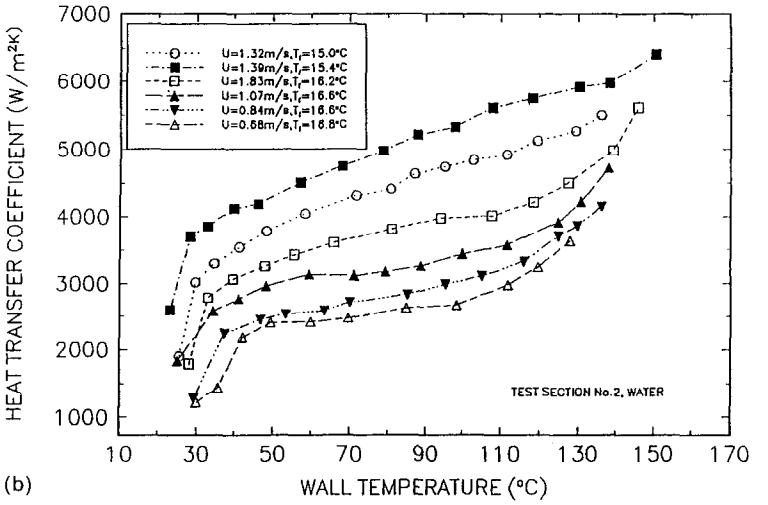

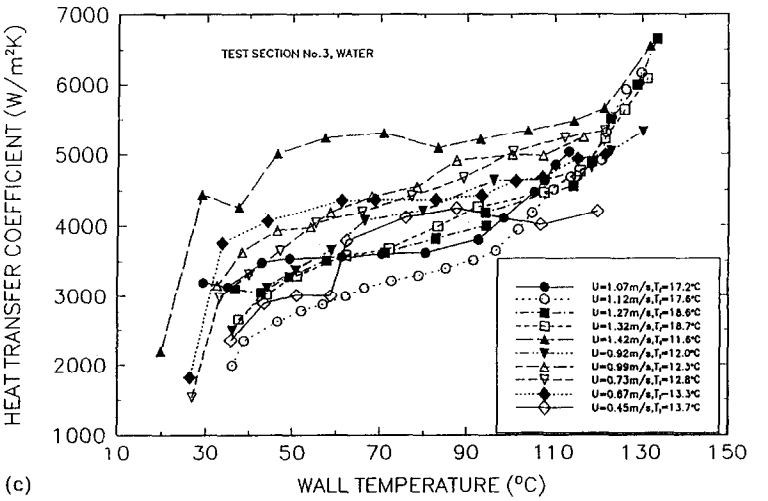

FIG. 3. Variation of heat transfer coefficient with wall temperature.

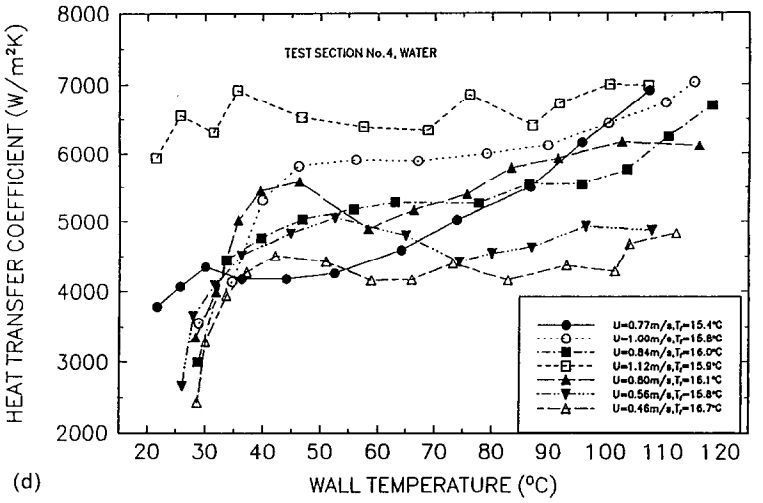

(d)

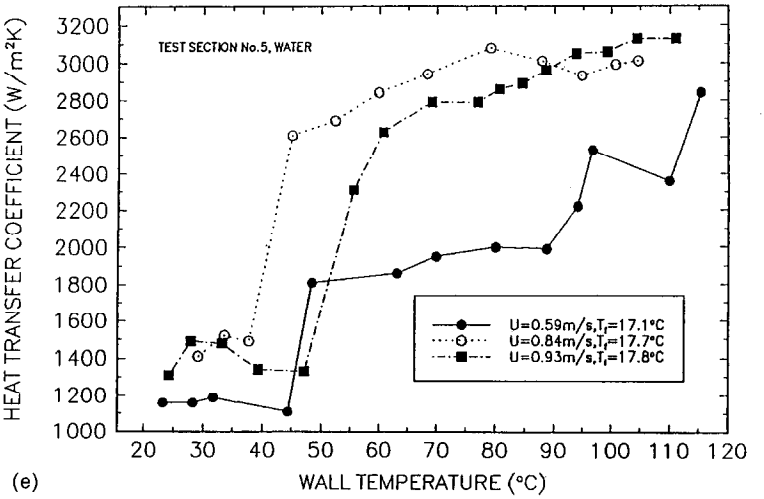

(e)

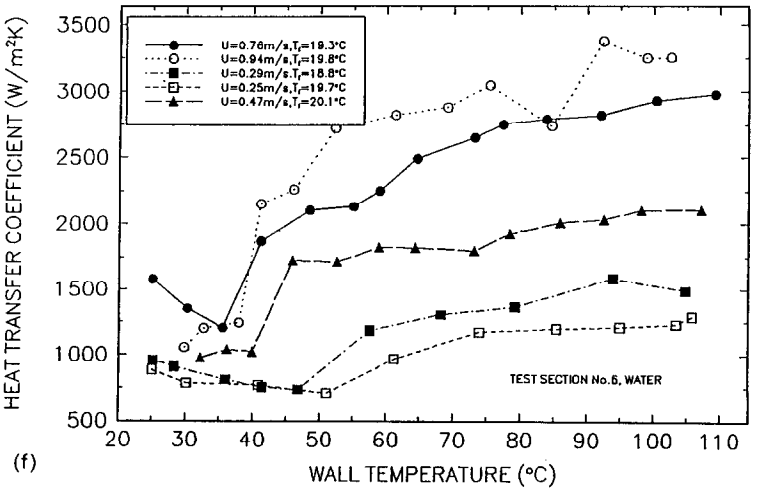

(f)

FIG. 3.—*Continued.*

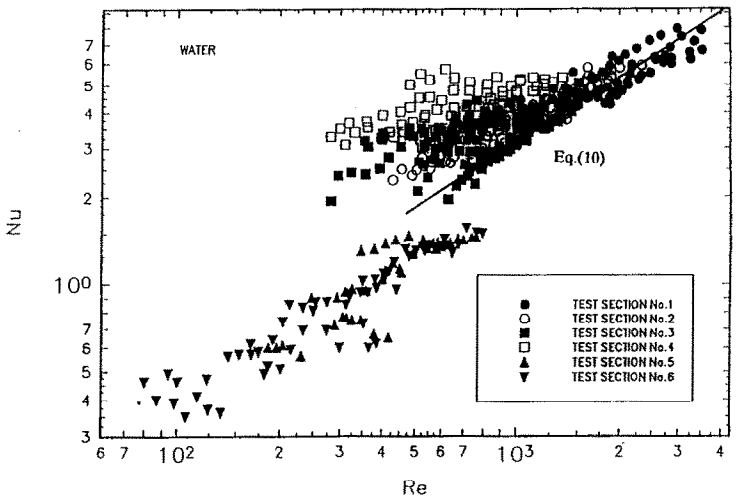

FIG. 4. Nusselt number vs Reynolds number for water.

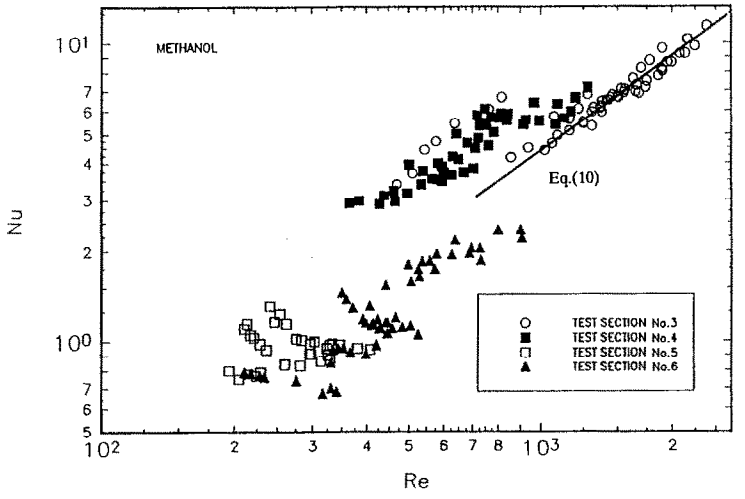

FIG. 5. Nusselt number vs Reynolds number for methanol.

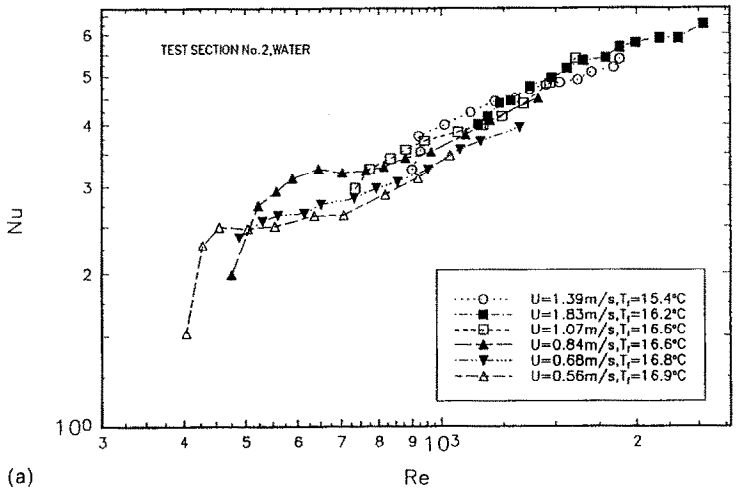

(a)

FIG. 6. Effects of liquid temperature and velocity.

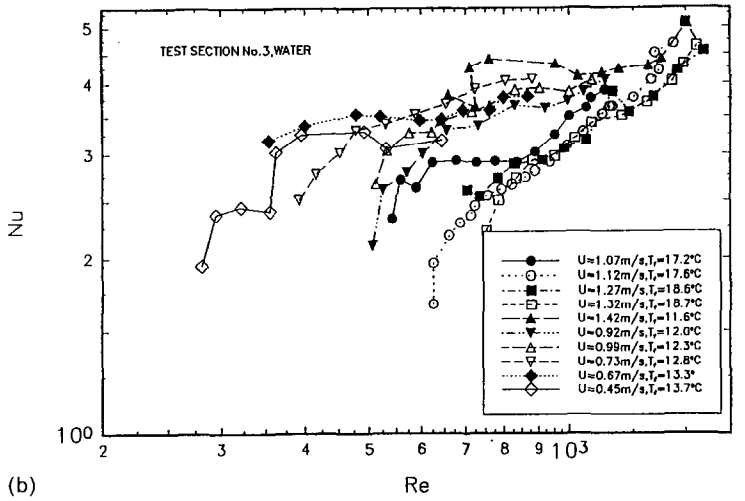

(b)

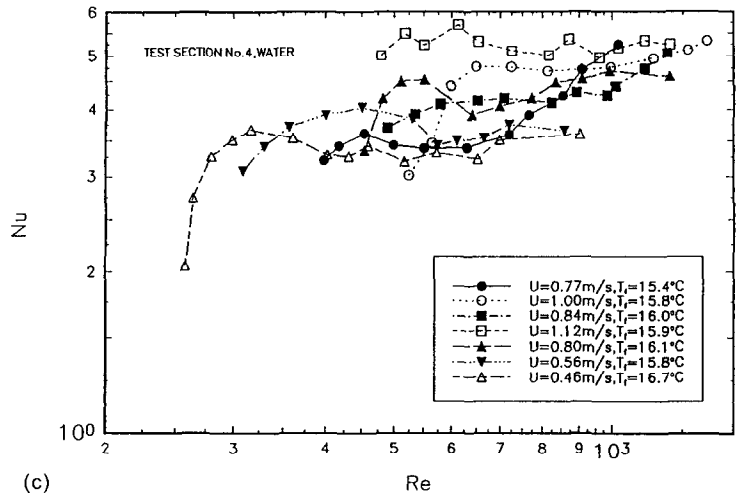

(c)

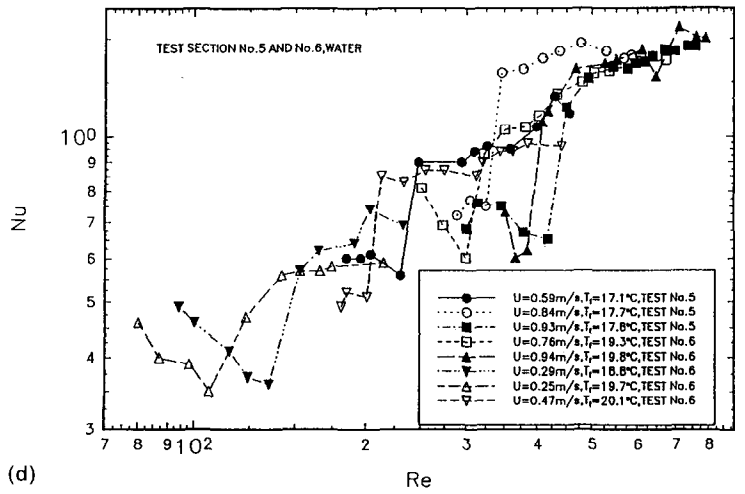

(d)

FIG. 6.—*Continued.*

known Dittus–Boelter equation was modified with the only difference of empirical constant, i.e. equation (10), to predict heat transfer; the results are in quite good agreement with experiment data for fully developed turbulent flow.

(2) Transition and laminar heat transfer in microchannels are highly strange and complicated, compared with the conventionally sized situation. The range of transition zone, and heat transfer characteristics of both transition and laminar flow are highly affected by liquid temperature, velocity and microchannel size.

REFERENCES

1. H. R. Jacobs and J. P. Hartnett, Thermal engineering: emerging technologies and critical phenomena, *A Report of the Future Needs for Thermal Engineering Research*, 1991, Workshop on Future Needs for Thermal Engineering Research sponsored by Natural Science Foundation and Pennsylvania State University (1991).
2. W. J. Yang and N. L. Zhang, Micro- and nano-scale heat transfer phenomena research trends. In *Transport Phenomena Science and Technology 1992* (Edited by B. X. Wang), pp. 1–15. Higher Education Press, Beijing (1992).
3. D. B. Tuckermann and R. F. Pease, High-performance heat sinking for VLSI, *IEEE Electronic Device Lett.* **2**(5), 126–129 (1991).
4. D. B. Tuckermann and R. F. Pease, Optimized convective cooling using micromachined structure, *J. Electrochem. Soc.* **129**(3), C98 (1982).
5. P. Y. Wu and W. A. Little, Measurement of friction factor for the flow of gases in very fine channels used for microminiature Joule–Thompson refrigerators, *Cryogenics* **24**(8), 273–277 (1983).
6. J. Pfahler, J. Harley, H. H. Bau and J. Zemel, Liquid transport in micron and submicron channels, *J. Sensors Actors* **A21–23**, 431–434 (1990).
7. S. B. Choi, R. F. Barron and R. O. Warrington, Liquid flow and heat transfer in microtubes. In *Micromechanical Sensors, Actuators and Systems* (Edited by D. Cho *et al.*), ASME DSC-Vol. 32, pp. 123–134 (1991).
8. B. R. Babin, G. P. Peterson and D. Wu, Steady-state modeling and testing of a micro heat pipe, *J. Heat Transfer* **112**(3), 595–601 (1990).
9. A. K. Mallik, G. P. Peterson and H. M. Weichold, On the use of micro heat pipes as an integral part of semiconductor devices, *Proceedings of the ASME/JSME Thermal Engineering Joint Conference*, Reno, Nevada, Vol. 2, pp. 393–401 (1991).
10. G. P. Peterson, A. B. Duncan, A. A. Ahmed, A. K. Mallik and M. H. Weichold, Experimental investigation of micro-heat pipe in silicon wasters, *Micromechanical Sensors, Actuators and Systems* (Edited by D. Cho *et al.*), ASME DSC-Vol. 32, pp. 341–348 (1991).
11. N. Zhang and W. J. Yang, Natural convection in evaporating minute drops, *J. Heat Transfer* **104**(3), 656–662 (1982).
12. N. Zhang and W. J. Yang, Evaporation and explosion of liquid drops on a heated surface, *Experiments in Fluids* **1**(1), 101–109 (1983).
13. N. Zhang, B. X. Wang and Y. Xu, Thermal stability of evaporating drops on a flat plate and its effect on evaporating rate, *Int. J Heat Mass Transfer* **30**(3), 469–478 (1989).
14. W. J. Yang, H. Takizwa and D. L. Vrable, Augmented boiling on copper–graphite composite surface, *Int. J. Heat Mass Transfer* **34**, 2751–2758 (1991).
15. L. Lin and A. P. Pisano, Bubble forming on a micro line heater, *Micromechanical Sensors, Actuators, and Systems* (Edited by D. Cho *et al.*), ASME DSC-Vol. 32, pp. 147–163 (1991).
16. X. F. Peng and B. X. Wang, Experimental investigation on flow boiling of liquid through microchannels, *(Chinese) J. Engng Thermophys.* (in Chinese, with English abstract) **14**(3), 281–286 (1993).
17. X. F. Peng and B. X. Wang, Forced convection and flow boiling heat transfer for liquid flowing through microchannels, *Int. J. Heat Mass Transfer* **34**, 3421–3427 (1993).
18. X. F. Peng and B. X. Wang, Forced convection for liquid methanol flowing through microchannels, *J. Thermal Sci.* (in press).